Local equilibrium and global relaxation of strained SiGe/Si(001) layers

M. Stoffel,[1,*] A. Rastelli,[1] J. Tersoff,[2] T. Merdzhanova,[1] and O. G. Schmidt[1]
[1]*Max-Planck-Institut für Festkörperforschung, Heisenbergstraße 1, 70569 Stuttgart-Germany*
[2]*IBM Research Division, T. J. Watson Research Center, Yorktown Heights, New York 10598, USA*
(Received 23 August 2006; published 27 October 2006)

We investigate the morphological evolution of islands obtained by epitaxial growth of Ge on Si(001) substrates. We are able to obtain highly uniform distributions of SiGe islands, which exhibit a "barn" shape. In addition to previously observed facets, we identify higher index facets, which are not observed in dome-shaped islands. The evolution of the island-related facet area provides evidence of a transition from domes to steeper barns, which continues the sequence of coherent island types before the onset of plastic relaxation. For higher Ge coverages, when plastically relaxed islands (superdomes) form, the island ensemble loses its homogeneity. This is essentially the result of anomalous coarsening, with material being transferred from coherent islands to larger superdomes.

DOI: 10.1103/PhysRevB.74.155326 PACS number(s): 81.15.Hi, 68.37.Ps, 68.47.Fg, 68.65.Hb

Strain-driven self-assembly represents nowadays the easiest route to fabricate semiconductor "quantum dots."[1] These structures have gained an increasing interest during the last decade mainly due to their potential application in future nanoscale electronic or optoelectronic devices.[2,3] In order to functionalize these structures in device architectures, it is important to control precisely their shape and size distribution. In most of the cases, a well-defined size with a small dispersion is required. The importance of size uniformity has already been addressed by several authors both experimentally and theoretically.[4–7] Among the different strained material combinations, the Ge/Si(001) system is the simplest. Due to the 4.2% lattice mismatch between Ge and Si, the growth follows the Stranski-Krastanow mode. The growth starts in a layer-by-layer mode up to a critical thickness of about 3-4 monolayers (ML). Then, at relatively high growth temperatures, the strain energy accumulated in the growing layer is partially relaxed through the formation of unfaceted mounds also called "prepyramids" on top of the wetting layer.[8–10] When the growth continues, the prepyramids transform into truncated pyramids and then into square-based pyramids or elongated hut clusters bounded by {105} facets.[11] A further increase of the Ge coverage leads to a transition from pyramids to dome islands bounded by steeper facets.[12] Finally, the dome islands may evolve into large, dislocated islands also called "superdomes."[13] This sequence of shape changes has been observed for the growth of $Si_{1-x}Ge_x$ on Si(001) (at least for $x>0.2$).[14] Recently, Sutter *et al.*[15] have identified a coherent island type, called "barn" because of its appearance in cross-sectional microscopy, during the deposition of dilute $Si_{1-x}Ge_x$ alloys ($x<0.2$) on Si(001) by gas-source molecular beam epitaxy. In addition to the commonly observed dome facets ({105}, {113} and {15 3 23}), {111} facets were identified on the barn surface.

In this paper, we show that coherent barns are also observed during growth of nominally pure Ge on Si(001) and delay the appearance of dislocated superdomes. We are able to obtain highly uniform distributions of SiGe islands that exhibit invariably a barn shape. This may affect the conclusions of models based on only two island shapes (pyramids and domes).[7,16] A careful analysis of their morphology allows us to identify high index facets, which were not recognized in Ref. 15. By measuring the coherent-island related facet areas, we provide evidence that the transition from domes to barns is very similar to the pyramid-to-dome transition, i.e., that the appearance of steeper facets is accompanied by a drop in the area of shallower facets.[13] By increasing the Ge coverage, plastic relaxation occurs in addition to the elastic relaxation. When superdomes appear, the aspect ratio of the coherent islands drops and their size distribution broadens essentially due to anomalous coarsening.[12] In fact, most of the deposited Ge is collected by the dislocated islands. We expect that material migration from small coherent islands towards superdomes allows for a global relaxation of the epilayer-plus-substrate system.

The samples were grown by solid source molecular beam epitaxy (MBE). After deoxidation at 950 °C, the substrate temperature was ramped down to 460 °C and a 100 nm thick Si buffer was deposited at a rate of 0.1 nm/s while ramping the temperature from 460 °C to 700 °C. After a 5 s growth interruption, 6 to 15 ML of Ge were grown at a rate of 0.04 ML/s. The samples were then cooled to room temperature immediately after growth at a rate of about 1 °C/s. The surface morphology was analyzed by *ex situ* atomic force microscopy (AFM) in tapping mode.

Figure 1 shows histograms of the island height obtained after deposition of 6 ML Ge [Fig. 1(a)], 8.5 ML Ge [Fig. 1(b)], 11 ML Ge [Fig. 1(c)], and 15 ML Ge [Fig. 1(d)] at 700 °C. The corresponding AFM images (2 μm$\times$2 μm) are shown in the insets. The color scale allows steep and shallow facets to be distinguished according to the local surface slope with respect to the (001) plane. If the growth is stopped at 6 ML Ge, the histogram reveals an inhomogeneous distribution with different island types. One can clearly recognize truncated pyramids, pyramids (P), islands with shape intermediate between pyramids and domes (TD) and domes (D),[16] where TDs and Ds are growing and smaller islands are in the process of shrinking.[10] In contrast, after deposition of 8.5 ML Ge, a highly uniform distribution of islands is obtained [Fig. 1(b)]. Such kind of distributions have already been observed by growing nominally pure Ge on Si(001) in the temperature range 620–750 °C.[6,17] In the last case, homoge-

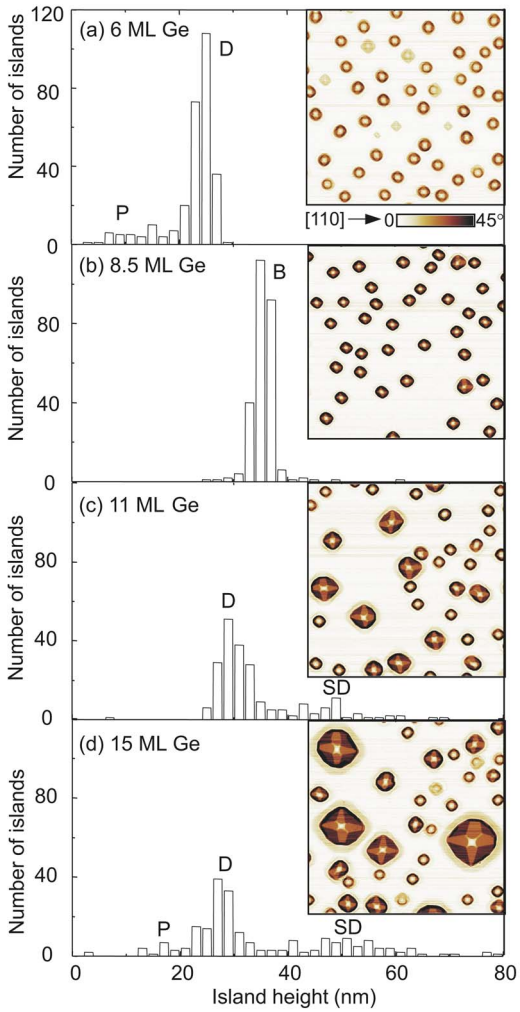

FIG. 1. (Color online) Histograms of the island height for different samples containing 6 ML Ge (a), 8.5 ML Ge (b), 11 ML Ge (c) and 15 ML Ge (d) deposited at 700 °C. The corresponding AFM images (2 μm × 2 μm) are shown in the insets.

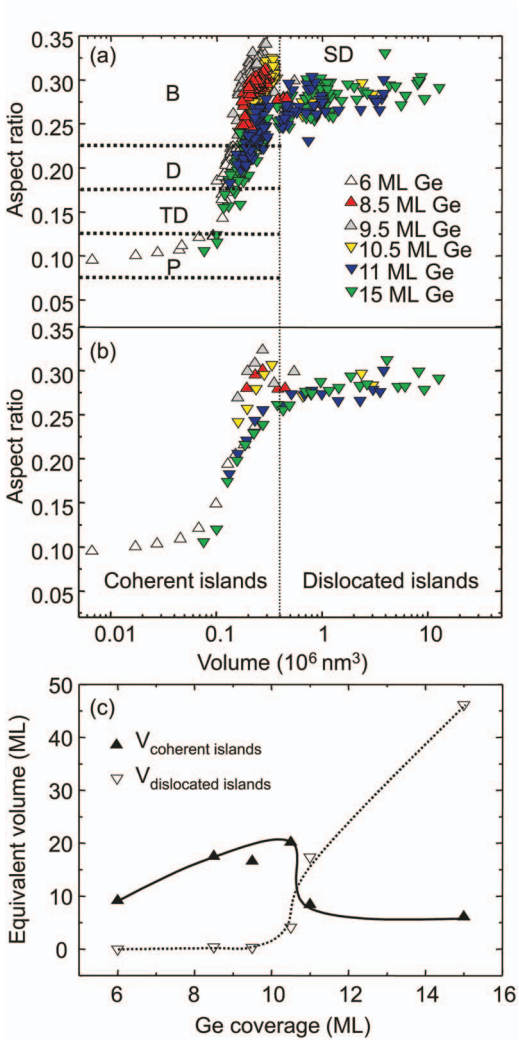

FIG. 2. (Color) (a) Evolution of the island aspect ratio versus volume for different samples with Ge coverages varying between 6 and 15 ML. The line marks the critical volume for dislocation introduction at 700 °C. (b) Average aspect ratio values for islands having similar volumes vs volume. (c) Evolution of the total volume per unit area incorporated in both coherent and dislocated islands vs Ge coverage.

neous size distributions were found (±5.5% height fluctuation).[17] At this stage, one can ask whether these islands are still dome islands. A qualitative comparison with the AFM image shown in the inset of Fig. 1(a) shows that the islands have much steeper facets than the well-known domes. We note that these islands are still coherent as revealed by transmission electron microscopy.[18] Due to their similarity with the islands already observed by Sutter *et al.*,[15] we will call them in the following "barns" (*B*). When the Ge coverage increases up to 11 ML [Fig. 1(c)], the island ensemble loses its homogeneity: dislocated superdome islands (*SD*) appear while coherent islands consist of shallower barns and domes. Finally, for a Ge coverage of 15 ML [Fig. 1(d)], a broad island distribution is obtained. The *SD*s become larger while the coherent islands consist of a distribution of shallow barns, domes, *TD*s and pyramids.

Figure 2(a) displays the aspect ratio versus volume for different Ge coverages between 6 and 15 ML. For clarity, we display the average aspect ratio values for islands having similar volumes in Fig. 2(b). For the lowest Ge deposition considered (6 ML), the aspect ratio values are distributed between 0.1 and 0.22. These are typical values for pyramids, *TD*s, and domes. In contrast, the aspect ratio values cluster around 0.3 for the sample containing 8.5 ML Ge [Fig. 2(a)], indicating that barns are indeed bounded by steeper facets than domes. The transition from dome to barn occurs via an increase of the island volume and height at approximately constant base area (not shown here). This suggests that domes transform into barns by accumulation of material at their top, similarly to the pyramid-to-dome transition.[19] When the Ge coverage increases to 9.5 ML, the aspect ratio increases slightly and the data points accumulate near the critical volume for dislocation introduction at 700 °C [marked by a line in Fig. 2(a)]. The latter is about 0.4 $\times 10^6$ nm^3 as determined by analyzing AFM images of the same surface area prior to and after selective SiGe etching.[20]

For higher Ge coverages of 11 and 15 ML, the aspect ratio of the coherent islands drops significantly with respect of the sample containing only 9.5 ML Ge. This indicates the gradual appearance of islands with intermediate shape between domes and mature barns, domes, and pyramids. Moreover, the drop of the coherent-island aspect ratio correlates with the appearance of large superdome islands on the film [see the AFM scans in Figs. 1(c) and 1(d)]. We can suggest here a possible scenario: when the Ge coverage increases, the largest barns evolve into superdomes containing dislocations and plastic relaxation occurs in addition to elastic relaxation. By evaluating the total volume per unit area contained in both coherent and dislocated islands [Fig. 2(c)], we find that the latter increases rapidly for Ge coverages higher than 10.5 ML. This observation suggests that the additional deposited Ge material flows essentially to the superdomes, which act as a sink for the Ge adatoms. Meanwhile, anomalous coarsening continues and material is transferred from small coherent islands to larger superdomes. This is supported by the presence of shrinking pyramids in the sample containing 15 ML Ge and by the decrease of the total volume incorporated in the coherent islands [Fig. 2(c)]. Consequently, the aspect ratio of coherent islands also decreases as shown in Figs. 2(a) and 2(b). We expect that material accumulation at the superdomes allows for a global relaxation of the epilayer-plus-substrate system. For dislocated islands, the aspect ratio values are scattered between 0.25 and 0.3. The superdome height increases monotonically with increasing base area as a result of their complex cyclic growth mode.[20,21] In the following, we will mainly focus our attention to the morphology of the barns. We have analyzed their facets following the procedure given in the literature.[13,22]

Figure 3 shows a typical barn island [Fig. 3(a)] and the corresponding facet plot averaged over many islands observed in several AFM images [Fig. 3(b)]. Apart from the {105}, the {113} and the {15 3 23} facets which have already been assigned to dome islands,[12,23] we can recognize additional spots that indicate the presence of steeper orientations. The presence of {111} facets has already been recognized by Sutter *et al.*[15] based on scanning tunneling and transmission electron microscopy. The additional spots can be identified by considering the known stable facets for Si and Ge[23,24] [see the stereographic plot in Fig. 3(d)]. We find that they are compatible with the presence of {20 4 23} facets. In order to directly compare this assignment with the experimental data, we build up a morphological model of the barn shape in three dimensions (3D) assuming the presence of these and the {111} facets close to the barn base and of the dome facets at the barn top, taking into account the experimental size from our AFM data. Two sets of eight facets belonging to the {20 4 23} family with slope of 41.9° [(±20 ±4 23) and (±4 ±20 23)] and 49.6° [(±23 ±4 20) and (±4 ±23 20)] are included in the model. The 3D view as well as a blurred two-dimensional (2D) image are shown in Figs. 3(c) and 3(e), respectively. The corresponding facet plot analysis [Fig. 3(f)] indicates that this construction is compatible with our experimental observations. The {20 4 23} facets, unnoticed in Ref. 15, were already observed at the base of superdomes.[13] Facets with compatible slope have also been observed in islands grown on prepatterned substrates.[25] Most important, it was shown that {20 4 23} facets define a major stable surface for Si,[24] but are not stable for pure Ge.[23,24] The origin and stability of these facets will be discussed later. We expect that even steeper facets and additional smaller facets could be present in the real shape but they cannot be resolved within the present study. Further investigations using high resolution scanning tunneling microscopy are needed to clarify this issue.

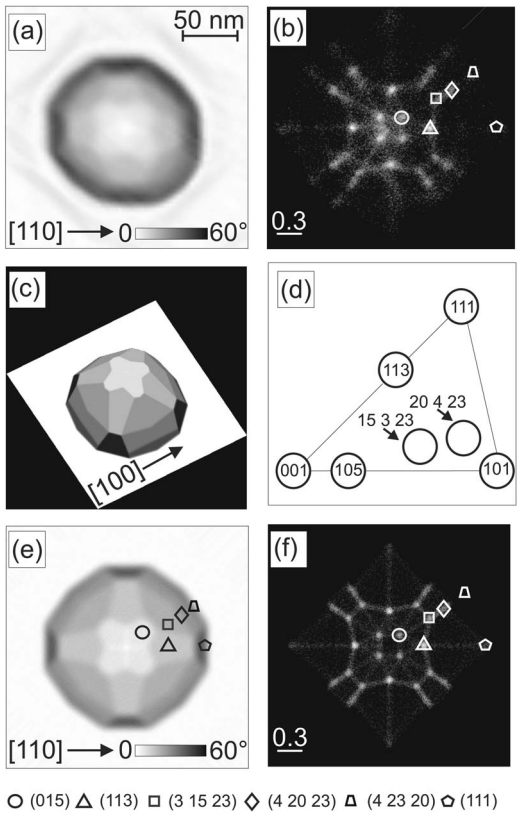

FIG. 3. (a) AFM scan (220 nm×220 nm) of a typical barn island. (b) Corresponding facet plot according to the method given in Refs. 13 and 22. The facets are labeled at the bottom. (c) 3D morphological model of a barn island. (d) Unit stereographic triangle of stable Ge(Si) surfaces. (e) Blurred image deduced from the 3D model. (f) Corresponding facet plot. Representative facets are labeled at the bottom.

In order to characterize the complete sequence of coherent island shapes observed during the growth of $Si_{1-x}Ge_x$ on Si(001), we compute, for each island, the area of each identified facet. We then group together the facets peculiar of each faceted shape, i.e., shallow facets ({105}), medium steepness facets ({113} and {15 3 23}), and steep facets ({111} and {20 4 23}). A scatter plot of the various facet areas versus island height is shown in Fig. 4. The islands with small heights are pyramids with shallow {105} facets. As the island size increases, the facet area obviously increases.[13] For islands higher than 15 nm, facets of medium steepness appear and the {105} facet area starts to drop, marking the pyramid-to-TD transition (marked by the left shaded area in Fig. 4). As observed in Ref. 13, the area of the {105} facets stays almost constant for mature domes, while the dome-related facets increase their extension. In our experiments, this con

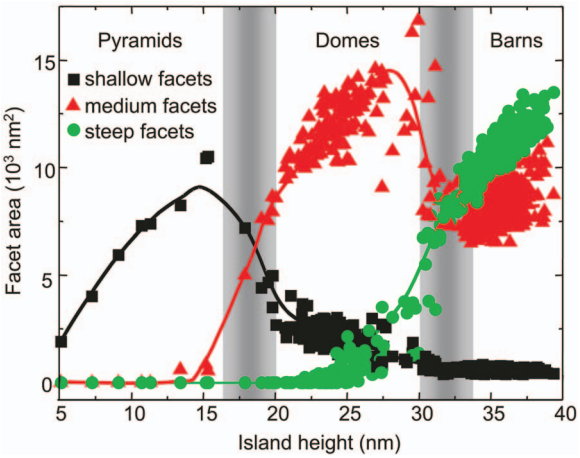

FIG. 4. (Color) Evolution of the islands related facet area vs island height. Shallow, medium, and steep facets indicate {105}, {113} and {15 3 23}, {20 4 23} and {111} facets, respectively. The lines are a guide for the eye. The shaded areas mark the transition from pyramids to domes and the transition from domes to barns.

tinues up to a height of 28 nm. For islands higher than 28 nm, steep facets appear and the medium slope facet area drops marking the dome-to-barn transition (marked by the right shaded area in Fig. 4). This result confirms that the transition from dome-to-barn behaves similarly to the pyramid-to-dome transition. Our analysis demonstrates that barns continue the sequence of coherent-island types before the formation of strain-relaxed superdomes. In the barn model shown in Fig. 3(c), we have assumed the presence of two sets of {20 4 23} facets with different slopes (see above). At this stage we cannot exclude that the barn morphology is actually the result of two subsequent transitions, each occurring when facets with increasing slope are introduced.

Finally, we discuss the origin and the stability of the barn shape. In an unfaceted continuum model,[26,27] it was shown that the aspect ratio increases monotonically for increasing island volumes. This is exactly what we observe experimentally in Figs. 2(a) and 2(b). A similar behavior is expected when the material is faceted except that instead of a smooth evolution, there are discrete transitions as newer and steeper facets are introduced.[14,28] The precise facets that will occur depend mainly on the surface energy and its dependence on both composition and strain. This trend is expected to continue until dislocation formation. We have shown that barns are bounded by additional {20 4 23} facets at their base, which define a major stable surface for Si.[24] Since we observe barns in the temperature range from 620 °C to 750 °C, where strong Si-Ge intermixing is known to occur,[17] we can speculate that the presence of a significant amount of Si is a necessary requirement for an island to reach the barn shape and delay the nucleation of dislocations. Compared to growth performed at lower temperatures, there is another remarkable difference, i.e., the presence of deep trenches around the island perimeters. Such trenches certainly alter the strain configuration of the islands and may play a role in stabilizing the {20 4 23} facets seen here.

In conclusion, we have characterized the morphological evolution of strained self-assembled SiGe islands. We can obtain monodisperse distributions of barn islands, which are bounded by steeper facets than dome islands. In addition to the facets already observed for dome islands, we identify {111} and {20 4 23} facets. The evolution of the islands facet area shows that the dome-to-barn transition has strong similarities to the well-characterized pyramid-to-dome transition. The barns are found to prolong the sequence of coherent-island shapes observed during growth of $Si_{1-x}Ge_x$ on Si(001). At higher Ge coverages, plastic relaxation of the epilayer occurs and the island size distribution broadens. This is the result of material transfer from coherent islands to superdomes and allows thus for a global relaxation of the epilayer-plus-substrate system. We expect that the island evolution reported here can be generalized to other strained material combinations.

This work was supported by the BMBF (No. 03N8711), the EU (No. 012150) and the DFG research group "Positioning of single nanostructures-single quantum devices". We acknowledge W. Yang for help in the assignment of the observed facets, K. von Klitzing for his continuous support and interest, and E. Coric for assistance in the AFM measurements.

*Electronic address: m.stoffel@fkf.mpg.de

[1] J. Stangl, V. Holý, and G. Bauer, Rev. Mod. Phys. **76**, 725 (2004).
[2] O. G. Schmidt and K. Eberl, IEEE Trans. Electron Devices **48**, 1175 (2001).
[3] Z. Yuan, B. E. Kardynal, R. M. Stevenson, A. J. Shields, C. J. Lobo, K. Cooper, N. S. Beattie, D. A. Ritchie, and M. Pepper, Science **295**, 102 (2002).
[4] T. I. Kamins, E. C. Carr, R. S. Williams, and S. J. Rosner, J. Appl. Phys. **81**, 211 (1997).
[5] F. M. Ross, J. Tersoff, and R. M. Tromp, Phys. Rev. Lett. **80**, 984 (1998).
[6] G. Jin, J. L. Liu, and K. L. Wang, Appl. Phys. Lett. **83**, 2847 (2003).
[7] R. E. Rudd, G. A. D. Briggs, A. P. Sutton, G. Medeiros-Ribeiro, and R. S. Williams, Phys. Rev. Lett. **90**, 146101 (2003).
[8] K. M. Chen, D. E. Jesson, S. J. Pennycook, T. Thundat, and R. J. Warmack, Phys. Rev. B **56**, R1700 (1997).
[9] A. Vailionis, B. Cho, G. Glass, P. Desjardins, D. G. Cahill, and J. E. Greene, Phys. Rev. Lett. **85**, 3672 (2000).
[10] A. Rastelli, M. Stoffel, J. Tersoff, G. S. Kar, and O. G. Schmidt, Phys. Rev. Lett. **95**, 026103 (2005).
[11] Y. W. Mo, D. E. Savage, B. S. Swartzentruber, and M. G. Lagally, Phys. Rev. Lett. **65**, 1020 (1990).
[12] F. M. Ross, R. M. Tromp, and M. C. Reuter, Science **286**, 1931 (1999).

[13] A. Rastelli and H. Von Känel, Surf. Sci. Lett. **515**, L493 (2002).
[14] A. Rastelli, H. Von Känel, B. J. Spencer, and J. Tersoff, Phys. Rev. B **68**, 115301 (2003).
[15] E. Sutter, P. Sutter, and J. E. Bernard, Appl. Phys. Lett. **84**, 2262 (2004).
[16] G. Medeiros-Ribeiro, A. M. Bratkovski, T. I. Kamins, D. A. A. Ohlberg, and R. S. Williams, Science **279**, 353 (1998).
[17] T. U. Schülli, M. Stoffel, A. Hesse, J. Stangl, R. T. Lechner, E. Wintersberger, M. Sztucki, T. H. Metzger, O. G. Schmidt, and G. Bauer, Phys. Rev. B **71**, 035326 (2005).
[18] N. Y. Jin-Phillipp (unpublished).
[19] F. Montalenti, P. Raiteri, D. B. Migas, H. Von Känel, A. Rastelli, C. Manzano, G. Costantini, U. Denker, O. G. Schmidt, K. Kern, and L. Miglio, Phys. Rev. Lett. **93**, 216102 (2004).
[20] T. Merdzhanova, S. Kiravittaya, A. Rastelli, M. Stoffel, U. Denker, and O. G. Schmidt, Phys. Rev. Lett. **96**, 226103 (2006).
[21] F. K. LeGoues, M. C. Reuter, J. Tersoff, M. Hammar, and R. M. Tromp, Phys. Rev. Lett. **73**, 300 (1994).
[22] C. Teichert, J. C. Bean, and M. G. Lagally, Appl. Phys. A **67**, 675 (1998).
[23] Z. Gai, X. Li, R. G. Zhao, and W. S. Yang, Phys. Rev. B **57**, R15060 (1998).
[24] Z. Gai, R. G. Zhao, W. Li, Y. Fujikawa, T. Sakurai, and W. S. Yang, Phys. Rev. B **64**, 125201 (2001).
[25] Z. Zhong, A. Halilovic, H. Lichtenberger, F. Schäffler, and G. Bauer, Physica E (Amsterdam) **23**, 243 (2004).
[26] B. J. Spencer and J. Tersoff, Phys. Rev. Lett. **79**, 4858 (1997).
[27] H. T. Johnson and L. B. Freund, J. Appl. Phys. **81**, 6081 (1997).
[28] J. Tersoff, B. J. Spencer, A. Rastelli, and H. Von Känel, Phys. Rev. Lett. **89**, 196104 (2002).